INES'2002- 6th International Conference on Intelligent Engineering Systems 2002, pg. 521-526, 26-29/May/2002, Opatija, Croatia.

Fractional Describing Function Analysis of Systems with Backlash and Impact Phenomena

R. S. Barbosa
Department of Electrotechnical Engineering
Institute of Engineering of Porto
Portugal
rbarbosa@dee.isep.ipp.pt

J. A. T. Machado
Department of Electrotechnical Engineering
Institute of Engineering of Porto
Portugal
jtm@dee.isep.ipp.pt

***Abstract* – This paper analyses the dynamical properties of systems with backlash and impact phenomena based on the describing function method. It is shown that this type of nonlinearity can be analyzed in the perspective of the fractional calculus theory. The fractional-order dynamics is illustrated using the Nyquist plot and the results are compared with those of standard models.**

I. INTRODUCTION

The area of Fractional Calculus (FC) deals with the operators of integration and differentiation to an arbitrary (including noninteger) order and is as old as the theory of classical differential calculus. The theory of FC is a well-adapted tool to the modelling of many physical phenomena, allowing the description to take into account some peculiarities that classical integer-order models simply neglect. For this reason, the first studies and applications involving FC had been developed in the domain of fundamental sciences, namely in physics [5] and chemistry [20]. Besides the intensive research carried out in the area of pure and applied mathematics [1–5], FC has found applications in various fields such as viscoelasticity/damping [6–12], chaos/fractals [13–14], biology [15], signal processing [16], system identification [17], diffusion and wave propagation [18], electromagnetism [19] and automatic control [21–25]. Nevertheless, in spite of the work that has been done in the area, the application of these concepts has been scarce until recently. In the last years, the advances in the theory of fractals and chaos revealed profound relations with FC, motivating a renewed interest in this field.

The phenomenon of vibration with impacts occurs in many branches of technology where it plays a very useful role. On the other hand, its occurrence is often undesirable, because it causes additional dynamic loads, as well as faulty operation of machines and devices. Despite many investigations that have been carried out so far, this phenomenon is not fully understood yet, mainly due to the considerable randomness and diversity of reasons underlying the energy dissipation involving the dynamic effects [28–32].

In this paper we investigate the dynamics of systems that contain backlash and impacts. It is shown that these nonlinear phenomena can exhibit a fractional-order dynamics and a chaotic behaviour revealing that FC is an adequate tool for the analysis of these systems.

Bearing these ideas in mind, the article is organized as follows. Sections 2 introduces the fundamental aspects of the describing function method. Section 3 studies the describing function of systems with backlash and impact phenomena. Finally, section 4 draws the main conclusions and addresses perspectives towards future developments.

II. DESCRIBING FUNCTION ANALYSIS

The describing function (DF) is one of the possible methods that can be adopted for the analysis of nonlinear systems [27]. The basic idea is to apply a sinusoidal signal in the input of the nonlinear element and to consider only the fundamental component of the signal appearing at the output of the nonlinear system. Then, the ratio of the corresponding phasors (output/input) of the two sinusoidal signals represents the DF of the nonlinear element. The use of this concept allows the adaptation of the Nyquist stability test to a nonlinear system detection of a limit cycle, namely the prediction of its approximate amplitude and frequency.

In this line of thought, we consider the control-loop with one nonlinear element depicted in Fig. 1.

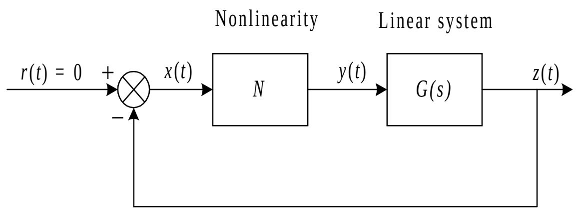

Fig. 1. Basic nonlinear feedback system for describing function analysis

We start by applying a sinusoid $x(t) = X\,\sin(\omega t)$ to the nonlinearity input. At steady-state the output of the nonlinear characteristic, $y(t)$, is periodic and, in general, it is nonsinusoidal. If we assume that the nonlinearity is symmetric with respect to the variation around zero, the Fourier series becomes:

$$y(t) = \sum_{k=1}^{\infty} Y_k \cos(k\omega t + \phi_k) \qquad (1)$$

where Y_k and ϕ_k are the amplidude and the phase shift of the k^{th}-harmonic component of the output $y(t)$, respectively.

In the DF analysis, we assume that only the fundamental harmonic component of $y(t)$, Y_1, is significant. Such assumption is often valid since the higher-harmonics in $y(t)$, Y_k for $k = 2, 3, \ldots$, are usually of smaller amplitude than the amplitude of the fundamental component Y_1. Moreover, most systems are "low-pass filters" with the result that the higher-harmonics are further attenuated.

Thus the DF of a nonlinear element, $N(X,\omega)$, is defined as the complex ratio of the fundamental harmonic component of output $y(t)$ with the input $x(t)$:

$$N(X,\omega) = \frac{Y_1}{X} e^{j\phi_1} \qquad (2)$$

where X is the amplitude of the input sinusoid $x(t)$ and Y_1 and ϕ_1 are the amplitude and the phase shift of the fundamental harmonic component of the output $y(t)$, respectively.

In general, $N(X,\omega)$ is a function of both the amplitude X and the frequency ω of the input sinusoid. For nonlinear systems that do not involve energy storage, the DF is merely amplitude-dependent, that is $N = N(X)$. If it is not the case, we may have to adopt a numerical approach because, usually, it is impossible to find a closed-form solution.

For the nonlinear control system of Fig. 1, we have a limit cycle if the sinusoid at the nonlinearity input regenerates itself in the loop, that is:

$$G(j\omega) = -\frac{1}{N(X,\omega)} \tag{3}$$

Note that (3) can be viewed as the characteristic equation of the nonlinear feedback system of Fig. 1. If (3) can be satisfied for some value of X and ω, a limit cycle is *predicted* for the nonlinear system. Moreover, since (3) applies only if the nonlinear system is in a steady-state limit cycle, the DF analysis predicts only the presence or the absence of a limit cycle and cannot be applied to analysis for other types of time responses.

III. ANALYSIS OF SYSTEMS WITH BACKLASH AND IMPACT PHENOMENA

In this section, we use the DF method to analyse systems with backlash and impact phenomena. We start by considering the standard static model and afterwards we study the case with the impact phenomena. Finally, we compare the results of the two types of approximations.

A. Static Backlash

Here, we consider the phenomena of clearance without the effect of the impacts, which is usually called *static backlash*.

The describing function for $X > h/2$ is given by [26]:

$$N(X) = \frac{k}{2}\left[1 - N_s\left(\frac{X/h}{1 - X/h}\right)\right] - j\,\frac{2kh(X - h/2)}{\pi X^2} \tag{4a}$$

$$N_s(z) = \frac{2}{\pi}\left[sin^{-1}\frac{1}{z} + \frac{1}{z}\cos\left(sin^{-1}\frac{1}{z}\right)\right] \tag{4b}$$

The classical backlash model corresponds to the DF of a linear system of a single mass M_1+M_2 followed by the geometric backlash having as input and as output the position variables $x(t)$ and $y(t)$, respectively, as depicted in Fig. 2.

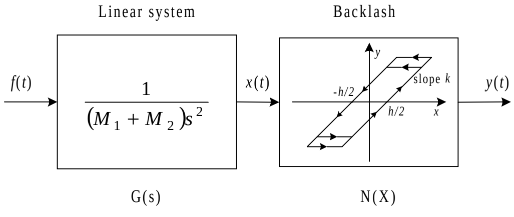

Fig. 2. Classical backlash model

For a sinusoidal input force $f(t) = F\cos(\omega t)$ the condition $X = h/2$ leads to the limit frequency ω_L applicable to this system:

$$\omega_L = \left[\frac{2}{h}\frac{F}{(M_1 + M_2)}\right]^{\frac{1}{2}} \tag{5}$$

Fig. 3 shows the Nyquist plot of $-1/N(F,\omega) = -1/[G(j\omega)N(X)]$ for several values of the input force F.

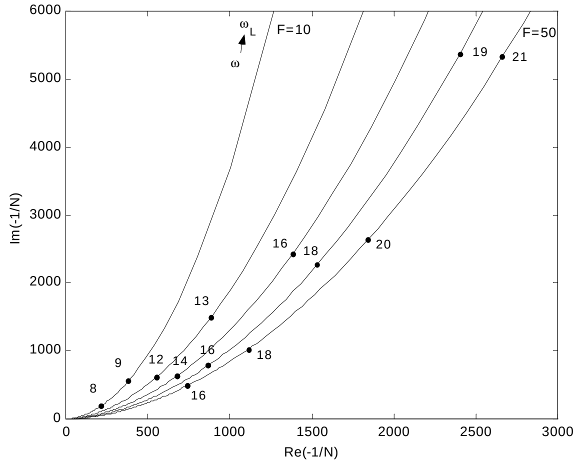

Fig. 3. Nyquist plot of $-1/N(F,\omega)$ for the system of Fig. 2, F = {10, 20, 30, 40, 50} N, $0 < \omega < \omega_L$, $M_1 = M_2 = 1$ kg and $h = 10^{-1}$ m

This approach to the backlash study is based on the adoption of a geometric model that neglects the dynamic phenomena involved during the impact process. Due to this reason often real results differ significantly from those predicted by that model.

B. Dynamic Backlash

In this section we use the DF method to analyse systems with backlash and impact phenomena, usually called *dynamic backlash*.

The proposed mechanical model consists on two masses (M_1 and M_2) subjected to backlash and impact phenomenon as shown in Fig. 4.

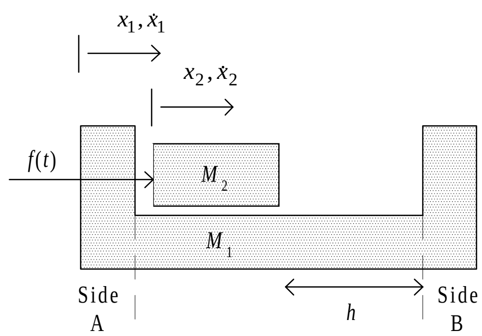

Fig. 4. System with two masses subjected to dynamic backlash

A collision between the masses M_1 and M_2 occurs when $x_1 = x_2$ or $x_2 = x_1+h$. In this case, we can compute the velocities of masses M_1 and M_2 after the impact ($\dot{x}_1'$ and $\dot{x}_2'$) by relating them to the previous values ($\dot{x}_1$ and $\dot{x}_2$) through the Newton's law:

$$(\dot{x}_1' - \dot{x}_2') = -\varepsilon\,(\dot{x}_1 - \dot{x}_2), \quad 0 \le \varepsilon \le 1 \tag{6}$$

where ε is the coefficient of restitution that represents the dynamic phenomenon occurring in the masses during the impact. In the case of a fully plastic (*inelastic*) collision

$\varepsilon = 0$, while in the *ideal elastic* case $\varepsilon = 1$.

The principle of conservation of momentum requires that the momentum, immediately before and immediately after the impact, must be equal:

$$M_1 \dot{x}_1' + M_2 \dot{x}_2' = M_1 \dot{x}_1 + M_2 \dot{x}_2 \tag{7}$$

From (6) and (7), we can find the sought velocities of both masses after an impact:

$$\dot{x}_1' = \frac{\dot{x}_1 (M_1 - \varepsilon M_2) + \dot{x}_2 (1+\varepsilon) M_2}{M_1 + M_2} \tag{8a}$$

$$\dot{x}_2' = \frac{\dot{x}_1 (1+\varepsilon) M_1 + \dot{x}_2 (M_2 - \varepsilon M_1)}{M_1 + M_2} \tag{8b}$$

The total kinetic energy loss E_L at an impact is determined by the relation:

$$E_L = \frac{1-\varepsilon^2}{2} \frac{M_1 M_2}{M_1 + M_2} (\dot{x}_1 - \dot{x}_2)^2 \tag{9}$$

For the system of Fig. 4 we can calculate numerically the Nyquist diagram of $-1/N(F,\omega)$ for an input force $f(t) = F\cos(\omega t)$ applied to mass M_2 while considering as output position $x_1(t)$ of mass M_1.

The values of the parameters adopted in the subsequent simulations are $M_1 = M_2 = 1$ kg and $h = 10^{-1}$ m. Figs. 5 and 6 show the Nyquist plots for $F = 50$ N and $\varepsilon = \{0.1, \ldots, 0.9\}$ and for $F = \{10, 20, 30, 40, 50\}$ N and $\varepsilon = \{0.2, 0.5, 0.8\}$, respectively.

The Nyquist charts of Figs. 5–6 reveal the occurrence of a jumping phenomenon, which is a characteristic of nonlinear systems. This phenomenon is more visible around $\varepsilon \approx 0.5$, while for the limiting cases ($\varepsilon \to 0$ and $\varepsilon \to 1$) the singularity disappears. Moreover, Fig. 6 shows also that for a fixed value of ε the charts are proportional to the input amplitude F.

The validity of the proposed model is restricted to frequencies of the exciting input force $f(t)$ higher than a lower-limit frequency ω_C. This frequency was determined numerically arriving to the approximate expression:

$$\omega_c \approx \left[\left(2 \frac{F}{M_2 \cdot h} \right)^2 \cdot (1-\varepsilon)^5 \right]^{\frac{1}{4}} \tag{10}$$

On the other hand, there is also an upper-limit frequency ω_L determined by application of Newton's law to mass M_2. Considering an input signal $f(t) = F\cos(\omega t)$ and solving for $x_2(t)$ we arrive at an expression for ω_L when the amplitude of the displacement is within the clearance $h/2$, yielding:

$$\omega_L = 2 \cdot \left(\frac{F}{h \cdot M_2} \right)^{\frac{1}{2}} \tag{11}$$

In the middle-range frequency, $\omega_C < \omega < \omega_L$, the jumping phenomena occurs at frequency ω_J that can be also obtained numerically having the relation:

$$\omega_J \sim \left(\frac{F}{h \cdot M_2} \right)^{\frac{1}{2}} \tag{12}$$

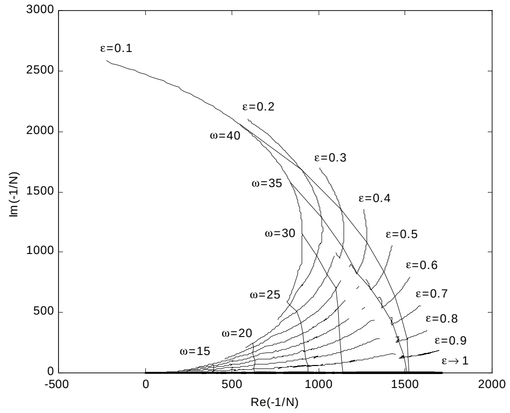

Fig. 5. Nyquist plot of $-1/N(F,\omega)$ for a system with dynamic backlash, $F = 50$ N and $\varepsilon = \{0.1, \ldots, 0.9\}$

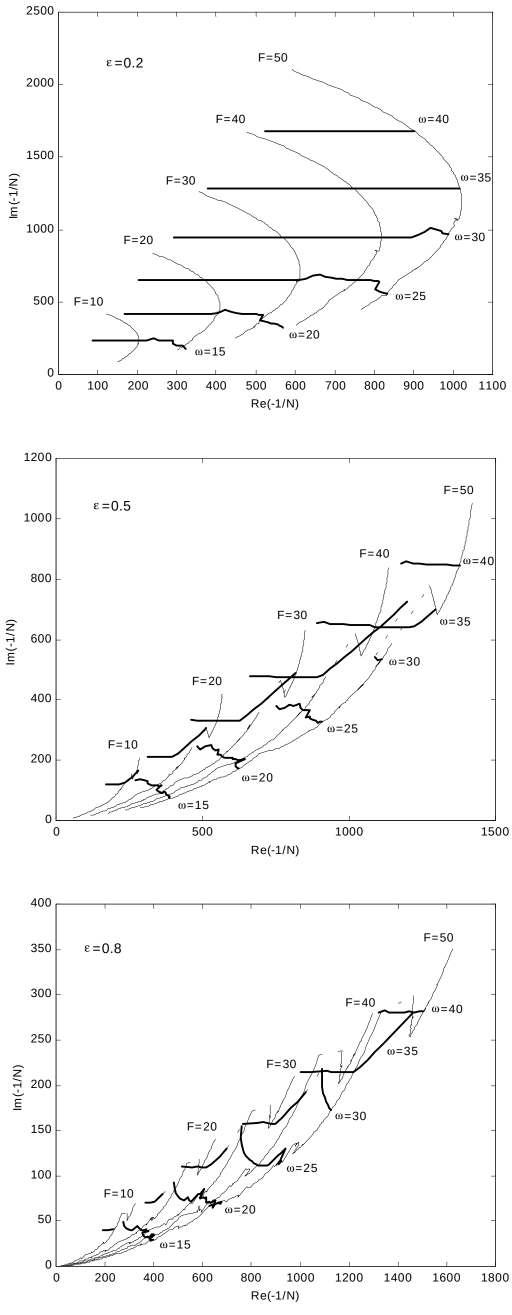

Fig. 6. Nyquist plot of $-1/N(F,\omega)$ for a system with dynamic backlash, $F = \{10, 20, 30, 40, 50\}$ N and $\varepsilon = \{0.2, 0.5, 0.8\}$

Figs. 7 and 8 illustrate the variation of the Nyquist plots of $-1/\mathrm{N}(F,\omega)$ for the cases of the static and dynamic backlash and shows the log-log plots of Re{−1/N} and Im{−1/N} *vs.* ω for a coefficient of restitution $\varepsilon = 0.5$ and F = {10, 20, 30, 40, 50} N and for an input force F = 50 N and ε = {0.1, 0.3, 0.5, 0.7, 0.9}, respectively.

Comparing the results for the static and the dynamic backlash models we conclude that:

- The charts of Re{−1/N} are similar for low frequencies (where they reveal a slope of +40 dB/dec) but differ significantly for high frequencies;
- The charts of Im{−1/N} are different in all range of frequencies. Moreover, for low frequencies, the dynamic backlash has a fractional slope inferior to +80 dB/dec of the static model.

A careful analysis must be taken because it was not demonstrated that a DF fractional slope would imply a fractional-order model. In fact, in this study we adopt integer-order models for the system description but the fractional-order slope is due to continuous/discrete dynamic variation that results due to the mass collisions.

A complementary perspective is revealed by Fig. 9 that depicts n_A (or n_B), the number of consecutive collisions on side A (or B), *vs.* the exciting frequency ω and the coefficient of restitution ε for an input force $f(t) = 50\cos(\omega t)$.

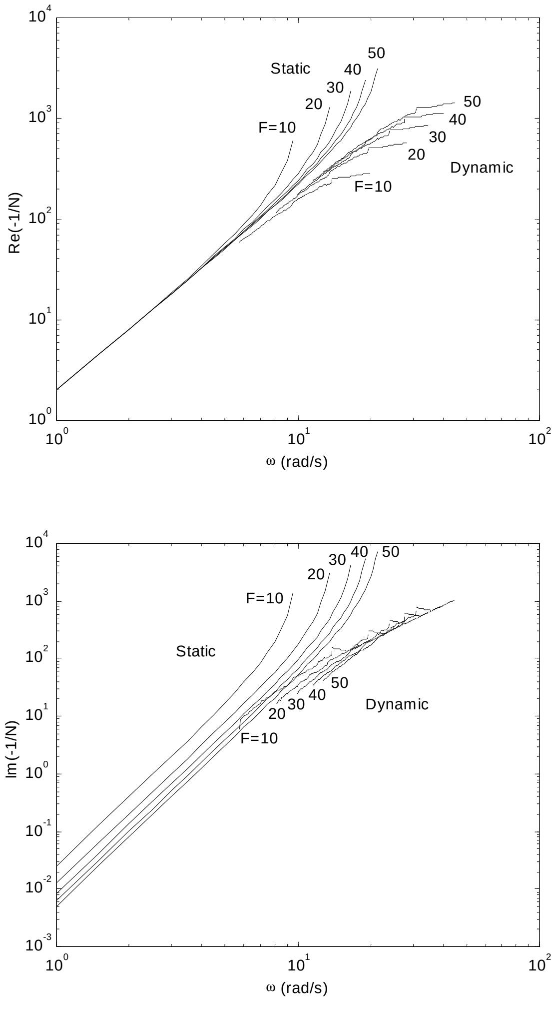

Fig. 7. Log-log plots of Re{−1/N} and Im{−1/N} *vs.* the exciting frequency ω, for ε = 0.5 and F = {10, 20, 30, 40, 50} N

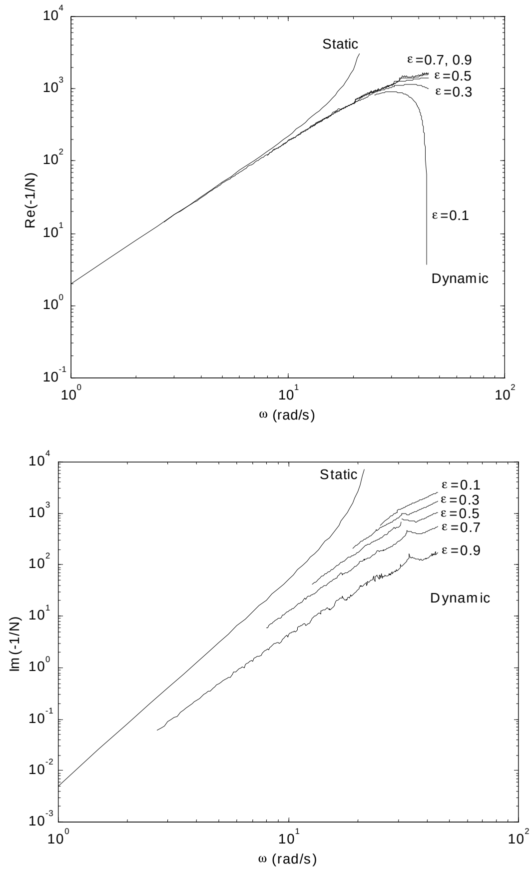

Fig. 8. Log-log plots of Re{−1/N} and Im{−1/N} vs. the exciting frequency ω, for F = 50 N and ε = {0.1, 0.3, 0.5, 0.7, 0.9}

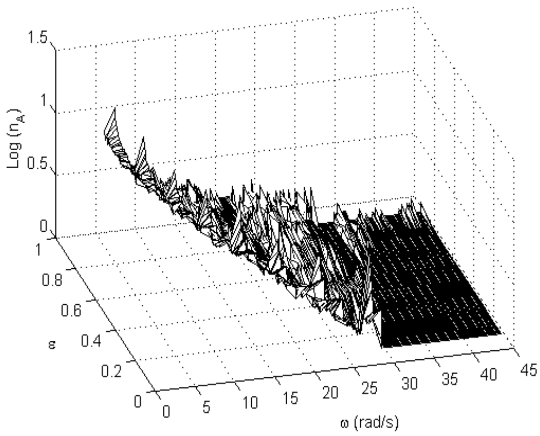

Fig. 9. Number of consecutive collisions on side A (n_A) *vs.* the exciting frequency ω and the coefficient of restitution ε, for an input force $f(t) = 50\cos(\omega t)$. For the side B (n_B) the chart is of the same type

From Fig. 9 we can distinguished two kinds of regions: the first, for $\omega_C < \omega < \omega_J$, where the system is characterized by an irregular number of impacts and a chaotic dynamics; the second, for $\omega_J < \omega < \omega_L$, where the motion is characterized by a regular behaviour corresponding to one alternate collision on each side of M_1.

Figs. 10–14 show the time response of the output velocity $\dot{x}_1(t)$ of a system with dynamic backlash for ω = {15, 20, 25, 35, 40} rad/s and ε = {0.2, 0.5, 0.8}. The charts lead to conclusion similar to those of Fig. 9, namely that we can have chaotic or periodic responses according with the values of ω and ε.

Model not applicable.
For ε = 0.2 it results a lower-limit frequency ω_c = 23.9 rad/s.

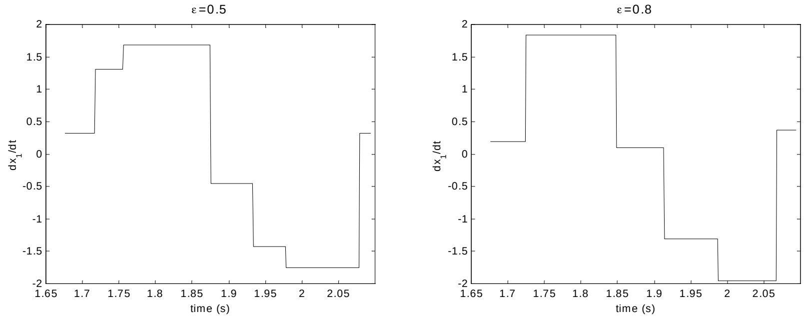

Fig. 10. Time response of the output velocity $\dot{x}_1(t)$ of the system with dynamic backlash, for an exciting frequency ω = 15 rad/s and ε = {0.2, 0.5, 0.8}

Model not applicable.
For ε = 0.2 it results a lower-limit frequency ω_c = 23.9 rad/s.

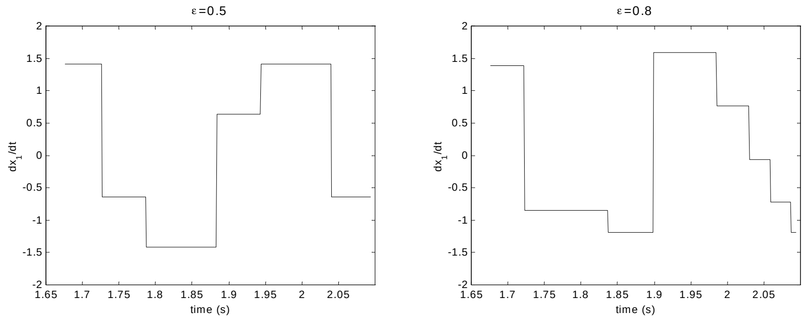

Fig. 11. Time response of the output velocity $\dot{x}_1(t)$ of the system with dynamic backlash, for an exciting frequency ω = 20 rad/s and ε = {0.2, 0.5, 0.8}

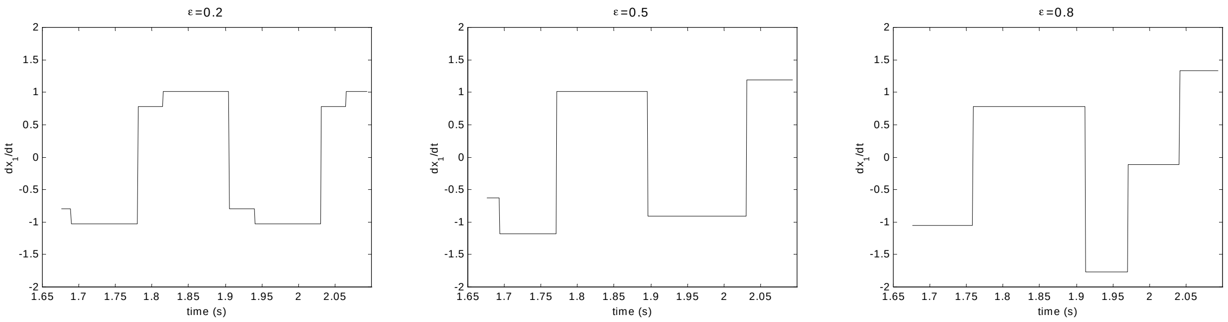

Fig. 12. Time response of the output velocity $\dot{x}_1(t)$ of the system with dynamic backlash, for an exciting frequency ω = 25 rad/s and ε = {0.2, 0.5, 0.8}

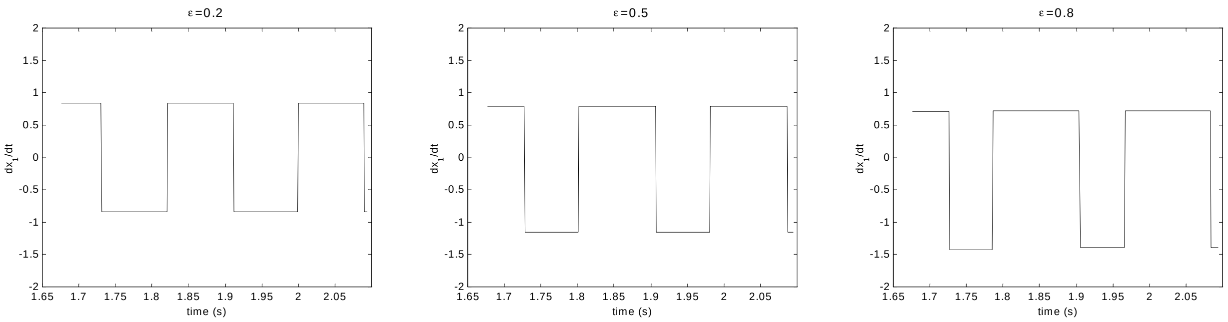

Fig. 13. Time response of the output velocity $\dot{x}_1(t)$ of the system with dynamic backlash, for an exciting frequency ω = 35 rad/s and ε = {0.2, 0.5, 0.8}

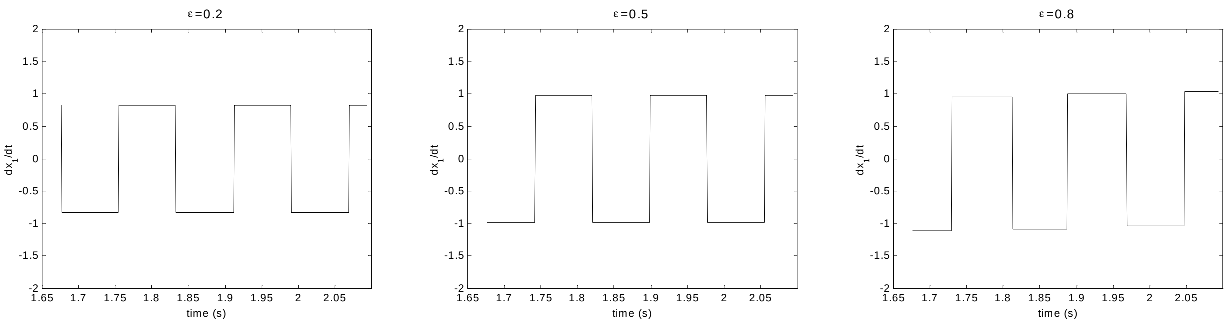

Fig. 14. Time response of the output velocity $\dot{x}_1(t)$ of the system with dynamic backlash, for an exciting frequency ω = 40 rad/s and ε = {0.2, 0.5, 0.8}

IV. CONCLUSIONS

This paper addressed several aspects of the phenomena involved in systems with backlash and impacts. The dynamics of a two-mass system was analysed through the describing function method and compared with standard models. The results revealed that these systems might lead to chaos and to fractional-order dynamics. These conclusions encourage further studies of nonlinear systems in the perspective of the fractional calculus since integer-order dynamical models are not capable to take into account many phenomena that occur.

V. REFERENCES

[1] K. B. Oldham and J. Spanier, *The Fractional Calculus*, Academic Press, New York: 1974.

[2] S. G. Samko, A. A. Kilbas and O. I. Marichev, *Fractional Integrals and Derivatives*, Gordon and Breach Science Publishers, Amsterdam: 1993.

[3] K. S. Miller and B. Ross, *An Introduction to the Fractional Calculus and Fractional Differential Equations*, John Wiley & Sons, New York: 1993.

[4] I. Podlubny, *Fractional Differential Equations*, Academic Press, San Diego: 1999.

[5] R. Hilfer, *Applications of Fractional Calculus in Physics*, World Scientific, Singapore: 2000.

[6] A. Gemant, “A Method of Analyzing Experimental Results Obtained from Elasto-Viscous Bodies,” *Physics*, vol. 7, 1936, pp. 311–317.

[7] R. L. Bagley and P. J. Torvik, “Fractional Calculus-A Different Approach to the Analysis of Viscoelastically Damped Structures,” *AIAA Journal*, vol. 21, no. 5, 1983, pp. 741–748.

[8] L. Rogers, “Operators and Fractional Derivatves for Viscoelastic Constitutive Equations,” *Journal of Rheology*, vol. 27, no. 4, 1983, pp. 351–372.

[9] R. C. Koeller, “Applications of Fractional Calculus to the Theory of Viscoelasticity,” *ASME Journal of Applied Mechanics*, vol. 51, 1984, pp. 299–307.

[10] N. Makris and M. C. Constantinou, “Fractional-Derivative Maxwell Model for Viscous Dampers,” *Journal of Structural Engineering*, vol. 117, no. 9, 1991, pp. 2708–2724.

[11] L. Gaul and M. Schanz, “Dynamics of Viscoelastic Solids Treated by Boundary Element Approaches in Time Domain,” *European Journal of Mechanics, A/Solids*, vol. 13, no. 4 – suppl., 1994, pp. 43–59.

[12] Åsa Fenander, “Modal Synthesis when Modeling Damping by Use of Fractional Derivatives,” *AIAA Journal*, vol. 34, no. 5, 1996, pp. 1051–1058.

[13] T. T. Hartley, C. F. Lorenzo and H. K. Qammer, “Chaos in Fractional Order Chua’s System,” *IEEE Transactions on Circuits and Systems-I: Fundamental Theory and Applications*, vol. 42, no. 8, 1995, pp. 485–490.

[14] A. Méhauté, *Fractal Geometries: Theory and Applications*, Penton Press, 1991.

[15] T. J. Anastasio, “The Fractional-Order Dynamics of Brainstem Vestibulo-oculomotor Neurons,” *Biological Cybernetics*, vol. 72, 1994, pp. 69–79.

[16] H. M. Ozaktas, Z. Zalevsky and M. A. Kutay, *The Fractional Fourier Transform*, John Wiley & Sons, Chichester: 2001.

[17] B. Mathieu, L. Le Lay and A. Oustaloup, “Identification of Non Integer Order Systems in the Time Domain,” in *IEEE SMC/IMACS Symposium on Control, Optimization and Supervision*, Lille, France, 1996, pp. 952–956.

[18] F. Mainardi, “Fractional Relaxation-Oscillation and Fractional Diffusion-Wave Phenomena,” *Chaos, Solitons & Fractals*, vol 7, no. 9, 1996, pp. 1461–1477.

[19] N. Engheta, “On the Role of Fractional Calculus in Electromagnetic Theory,” *IEEE Antennas and Propagation Magazine*, vol. 39, no. 4, 1997, pp. 35–46.

[20] A. Méhauté, ‘’From Dissipative and to Non-dissipative Processes in Fractal Geometry: The Janals,” *New Journal of Chemistry*, vol 14, no. 3, 1990, pp. 207–215.

[21] A. Oustaloup, *La Commande CRONE: Commande Robuste d’Ordre Non Entier*, Hermes, Paris: 1991.

[22] J. A. Tenreiro Machado, “Analysis and Design of Fractional-Order Digital Control Systems,” *SAMS Journal Systems Analysis, Modelling, Simulation*, vol. 27, 1997, pp. 107–122.

[23] J. A. Tenreiro Machado, “Discrete-Time Fractional-Order Controllers”, *FCAA Fractional Calculus and Applied Analysis*, vol. 4, no. 1, 2001, pp. 47–66.

[24] B. M. Vinagre, I. Podlubny, A. Hernández and V. Feliu, “Some Approximations of Fractional Order Operators Used in Control Theory and Applications,” *FCAA Fractional Calculus and Applied Analysis*, vol. 3, no. 3, , 2000, pp. 231–248.

[25] I. Podlubny, “Fractional-Order Systems and $PI^{\lambda}D^{\mu}$ - Controllers,” *IEEE Transactions on Automatic Control*, vol. 44, no. 1, 1999, pp. 208–213.

[26] C. L. Phillips and R. D. Harbor, *Feedback Control Systems*, Prentice-Hall, 1991.

[27] J. E. Slotine and W. Li, *Applied Nonlinear Control*, Prentice-Hall, 1991.

[28] A. Azenha and J. A. T. Machado, “On the Describing Function Method and the Prediction of limit Cycles in Nonlinear Dynamical Systems,” *SAMS Journal of Systems analysis, Modelling and Simulation*, vol. 33, 1998, pp. 307–320.

[29] G. Tao and P. V. Kokotovic, “Adaptive Control of Systems with Unknown Output Backlash,” *IEEE Transactions on Automatic Control*, vol. 40, no. 2, 1995, pp. 326–330.

[30] Y. S. Choi and S. T. Noah, “Periodic Response of a Link Coupling with Clearance,” *ASME Journal of Dynamic Systems, Measurement and Control*, vol. 111, no. 2, 1989, pp. 253–259.

[31] S. Dubowsky, J. F. Deck and H. Costello, “The Dynamic Modelling of Flexible Spatial Machine Systems with Clearance Connections,” *ASME Journal of Mechanisms, Transmissions and Automation in Design*, vol. 109, no. 1, 1987, pp. 87–94.

[32] Y. Stepanenko and T. S. Sankar, “Vibro-Impact Analysis of Control Systems with Mechanical Clearance and Its Application to Robotic Actuators,” *ASME Journal of Dynamic Systems, Measurement and Control*, vol. 108, no. 1, 1986, pp. 9–16.